

Frequency-dependent conductivity of a strongly disordered two-dimensional electron gas

A. Gold

Physik Department, Technische Universität München, D 8046 Garching, Germany

S. J. Allen, B. A. Wilson, and D. C. Tsui
Bell Laboratories, Murray Hill, New Jersey 07974
 (Received 24 August 1981)

We compare the predictions of Götze's theory for the strongly disordered two-dimensional electron gas based on a self-consistent current-relaxation kernel with experimental temperature and frequency-dependent conductivities $\sigma(T, \omega)$ measured in n inversion layers on Si(100) surfaces. With a unique value for the strength and range of the random potential one can achieve a convincing fit to both $\sigma(T, \omega=0)$ and $\sigma(T=0, \omega)$ over a range of electron densities that span the "metal"-insulator transition. The satisfactory agreement is conditional on the assumption that the valley degeneracy is lifted.

I. INTRODUCTION

A recent theory of the Anderson transition in strongly disordered systems put forward by Götze¹⁻³ focuses on the self-consistent determination of the "memory function" or current-relaxation kernel, $M(\omega)$. As the relative strength of the disorder and Fermi energy of the noninteracting particles is varied, the memory function is shown to exhibit a crossover from conducting to insulating behavior. The theory is capable of making quantitative predictions of the electron transport with only the electron density and mass, and disordering potential strength and range as input parameters. The results have been successfully applied to some three-dimensional systems by Belitz and Götze.⁴

In two dimensions (2D) the problem of localization is rendered more interesting by the fact that there appears to be no true metallic conduction.⁵⁻⁷ In 2D the transition is rather between a weakly, logarithmically, localized state to a strongly, exponentially, localized state.⁵ Although the present theory is not capable of dealing with the weakly localized regime^{8,9} it appears to have success in quantitatively describing the transition to strong localization. In the work of Gold and Götze¹⁰ for 2D systems the weakly localized regime is treated as metallic and the transition to strong localized regime is found to depend on the strength and range of the random potential. Satisfactory fits were obtained to a number of experiments¹¹⁻¹³ on 2D conductivity in the strongly localized regime.

Considerable support was given to Pepper's¹⁴ idea that the quantitative differences in conductivity scale on which localization was observed could be understood by different length scales for the random potential.

The key quantity is the current-relaxation kernel which directly determines the frequency-dependent conductivity. Conversely, the frequency-dependent conductivity can be used to determine the real and imaginary parts of the current-relaxation kernel (at least at $q=0$) and provides us with an independent test of the applicability of this approach to localization.

In the following we compare measurements of the temperature- and frequency-dependent conductivity of 2D electron gas found in Si inversion layers with the predictions of the self-consistent current-relaxation theory. We also extract from the experimental data the real and imaginary current-relaxation kernel and compare this with the theory as well.

The theoretical basis for the fits to the temperature- and frequency-dependent conductivity is discussed in Sec. II. The experimental details and results are exposed in Sec. III, followed by discussion and conclusions in Secs. IV and V.

II. THEORY

The central concept of the theory is a current-relaxation kernel M , a function of frequency ω , and various parameters specifying the Hamiltoni-

an. This kernel determines the dynamical conductivity for zero temperature and Fermi energy ϵ via a generalized Drude formula

$$\sigma_\epsilon(\omega) = \frac{n_s e^2}{m} g_s g_v \frac{i}{\omega + M(\omega)}, \quad (1)$$

where n_s is the electron density per spin, e is the electron charge, m the effective mass of the electron, and g_s, g_v the spin and valley degeneracy. The kernel $M(\omega)$ is causal function meaning that $M''(\omega)$ and $M'(\omega)$ are connected by the Kramers-Kronig relation and $M''(\omega) \geq 0$. Thus, $M''(\omega)$ describes relaxation effects, while $M'(\omega)$ describes memory effects.

From a theoretical point of view the function $M(\omega)$ is simpler than $\sigma_\epsilon(\omega)$ and does not directly reflect the trivial free motion but describes the spectrum of the random forces acting on the electrons. For free motion $M(\omega) = 0$, while σ_ϵ has a simple pole $\sigma_\epsilon \sim i/\omega$. In weakly perturbed systems, as in ordinary metals, $M(\omega)$ may be evaluated by a straightforward perturbation expansion.

In strongly disordered systems, where the mean free path attains the order of the de Broglie wavelength, the current-relaxation spectrum has to be calculated self-consistently with the propagation of electron-density perturbations. The latter are described by

$$\phi(q, \omega) = \frac{\phi^0(q, \omega + M(\omega))}{1 + M(\omega)\phi^0(q, \omega + M(\omega))/K(q)} \quad (2)$$

and

$$M(\omega) = \frac{U^2}{nmq_0^2} \int_0^{q_0} dq q^3 \phi(q, \omega), \quad (3)$$

where we have used a white-noise model for the fluctuating potential which is specified by two parameters, a strength U and a cutoff q_0 [$U(q)U(-q) = 4\pi U^2/q_0^2 \Theta(q_0 - q)$, $\langle U(q) \rangle = 0$]. The properties of the electron gas m, ϵ enter via the free gas density correlation function $\phi^0(q, z)$, which depends on wave vector q and complex frequency z and is given by the free gas compressibility $K(q, z)$ (Ref. 15) and the static limit $K(q) = K(q, z = 0)$ (Ref. 15)

$$\phi^0(q, z) = \frac{1}{z} [K(q, z) - K(q)]. \quad (4)$$

Equations (2), (3), and (4) define a transcendental equation for $M(\omega)$, which can be solved in a straightforward manner by a Newton iteration procedure. So, for fixed m, ϵ, U , and q_0 one obtains the relaxation kernel $M(\omega)$ and then with (1) the

desired conductivity.

The Kubo-Greenwood formula gives the temperature-dependent conductivity

$$\sigma(T, \omega) = \int d\epsilon \sigma_\epsilon(\omega) \frac{1}{4T \cosh^2 \left[\frac{\epsilon - \mu}{2k_B T} \right]}, \quad (5)$$

where μ is the chemical potential, T is the temperature, and k_B the Boltzmann constant.

The theory exhibits a metal-insulator transition as the potential strength becomes greater than a critical value with fixed density and an insulator-metal transition when the Fermi energy becomes greater than a critical value (localization edge). This behavior was proposed in experiments with n inversion layers on Si surfaces.¹¹⁻¹⁴

In the conductor phase $M''(\omega)$ is regular and $M''(\omega) > 0$, while $M'(\omega)$ goes to zero for $\omega \rightarrow 0$. The frequency dependence of $M'(\omega)$ is the origin of precursor phenomena in $\sigma'_\epsilon(\omega)$. Near the localization edge $\sigma'_\epsilon(\omega = 0) > 0$, but the maximum of $\sigma'_\epsilon(\omega)$ is at a finite frequency. Therefore, the frequency dependence of $\sigma'_\epsilon(\omega)$ is non-Drude-like and is like one of an over-damped oscillator. In the insulator regime $M'(\omega)$ has a simple pole $M'(\omega) \sim 1/\omega$ for $\omega \rightarrow 0$ and $\sigma'_\epsilon(\omega)$ is zero for $\omega \rightarrow 0$ and has a maximum for a finite frequency.

For detailed discussion of the approximations leading to the self-consistent equations (2) and (3) and the properties of the solution, we refer to the quoted papers, Refs. 3 and 10. Please note that it is clear from Eq. (2) that the theory fulfills the compressibility and the f sum rule.

III. EXPERIMENT

The experimental objective of this work is the simultaneous measurement of the temperature dependence of the dc conductivity, $\sigma'(T, \omega = 0)$, of the 2D electron gas found in Si inversion layers and the frequency dependence of the same conductivity with the temperature held at some low temperature, $\sigma'(T, 0, \omega)$. Within the framework of the theoretical model that follows, we make take T as near zero. While the dc conductivity may be probed as a function of temperature with efficacy the frequency dependence can be obtained only after much time consuming signal averaging. As a result, dc conductivity and high-frequency conductivity were obtained only on a limited number of samples. The characteristics of these samples are documented in Table I.

TABLE I. Sample characteristics.

Sample	Orientation	Peak mobility at 4.2 K $\text{cm}^2/(\text{V s})$ [at n_s (cm^{-2})]	Oxide thickness (\AA)	P-type substrate doping (cm^{-3})	Fixed oxide charge (cm^{-2})	Gate oxidation
1	100	16 000 [2.4×10^{11}]	5230	1.3×10^{15}	4×10^{10}	wet
2	100	12 000 [9.3×10^{11}]	3680	1.2×10^{15}	4×10^{10}	wet
3	100	16 000 [6.8×10^{11}]	1220	1.0×10^{15}	-4×10^{10}	dry
4	100	16 000 [6.8×10^{11}]	1220	1×10^{15}	-4×10^{10}	dry
5	100	4500 [8×10^{11}]	1425	0.7×10^{15}	$+ 10 \times 10^{10}$	wet

Detailed results were obtained on one, sample no. 1, which we have found representative of high peak mobility ($\geq 10\,000 \text{ cm}^2/\text{V sec}$), [100]-oriented n -channel devices, and we document these here. (The last sample in Table I does not have high peak mobility at 4.2 K but is listed as it was the basis of an earlier publication.¹⁶)

The device geometry is shown in Fig. 1. Large square devices were used with semitransparent gates to facilitate transmission of far-infrared radiation. Two- and four-terminal measurements were performed as a function of temperature at various electron densities and reverse substrate bias.

The infrared conductivity was determined from the following expression:

$$\text{Re}[\sigma(\omega)] = \sigma'(\omega) = \frac{1}{2}(\Delta T/T)(Y_0 + Y_{\text{Si}} + Y_{\text{gate}}). \quad (6)$$

$\Delta T/T$ is the fractional change in transmission caused by introducing the inversion layer electrons (see Fig. 2). $\text{Re}(\sigma) = \sigma'(\omega)$ is the real conductivity and Y_0 , Y_{Si} , and Y_{gate} are the wave admittance of free space, the silicon substrate, and the gate metallization. The technique has been described elsewhere.¹⁷

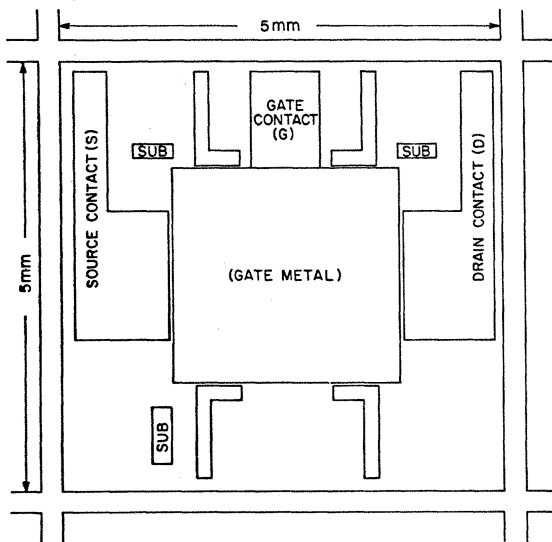


FIG. 1. Planar view of metallization on Si-metal-oxide-semiconductor field-effect transition.

A. dc conductivity versus temperature

Frequently, high-peak-mobility devices on (100) surfaces have contact resistance at low electron densities and low temperatures that mask the true conductance of the inversion layer. Remarkably, a large negative substrate bias remedies the problem and the two-terminal source and drain measurement can be shown to give reliable measurement of conductivity. Although this contact problem occurs frequently in high-mobility devices, we documented its pathology elsewhere since it is tangential to the main effort here. Suffice it to say that the results quoted below are not comprised by contact effects. (It is possible that the dc measurements reported earlier¹⁶ were in error due to contact problems. The high-frequency measurements needless to say were contact-free.)

The threshold was determined by extrapolating the broad-band infrared absorption ($5-50 \text{ cm}^{-1}$)

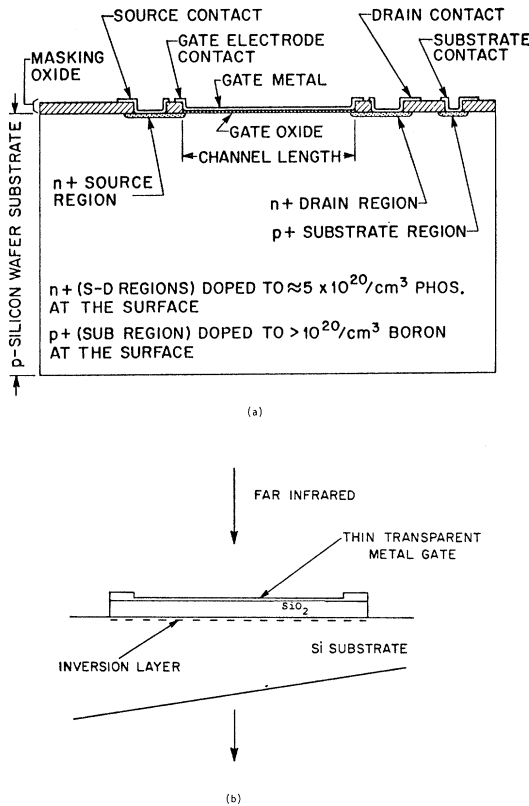


FIG. 2. (a) Cross section through a typical device. (b) Schematic cross section indicating relevant media that interact with far-infrared radiation.

to zero as the gate voltage was varied. This has been shown to give threshold to within $\pm 10^{10}/\text{cm}^2$ in devices that have no long-term hysteresis at low temperature and equilibrate quickly (1 sec) as the gate voltage is changed. The latter is facilitated by switching the gate voltage from the value of interest to just below threshold. In this way the depletion layer, which may charge or discharge slowly, is left intact. In well-behaved devices the threshold determined by infrared absorption agrees with the 77-K conductivity threshold and the threshold determined from Shubnikov-de Haas oscillations^{18,19} within $\pm 10^{10}/\text{cm}^2$.

It should be noted that the threshold shifts induced at temperatures of 77 K and below by a reverse substrate bias were substantially smaller than those predicted from the known substrate doping. Under these circumstances we disregard the applied substrate voltage and used the threshold shift itself as a measure of the depletion layer field. Despite the lack of agreement between measured and predicted threshold shift the depletion layer field equilibrated rapidly (< 1 sec) down to the

lowest temperatures used (1.2 K). The field distribution was uniform to within the estimated uncertainty in the electron density ($\pm 10^{10}/\text{cm}^2$). We conclude that the depletion layer quickly equilibrates to a potential that is less than the applied substrate potential because of a potential drop in the high resistivity substrate at low temperatures. Although this anomaly in the depletion layer field is not understood it does not comprise the interpretation of the experiment.

In Fig. 3 we show the measured dc conductance as a function of temperature with a reverse substrate bias of -10 V. At high electron densities the conductance is "metallic" whereas at low electron densities the conductance is localized showing activation energies of the order of meV at the lowest electron density.

Note that we are not concerned here with the weak logarithmic localization that has recently been reported in these devices.⁷ In the temperature range of our measurements (> 1.2 K) and within the precision with which we view these results (5%), weak localization only becomes apparent in the threshold region ($\sigma \sim 10^{-4}$ mho/ \square). At higher conductivity the system is essentially metallic and lower conductivity strongly localized by disorder. The transport is essentially Ohmic for electric

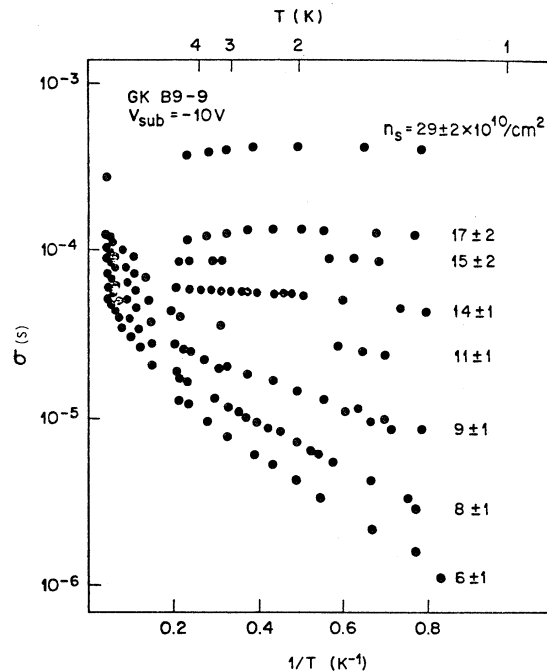


FIG. 3. Conductivity vs temperature for sample no. 1, -10 V substrate bias applied.

fields below which pinch-off or enhancement is caused by the source drain field. The exception to this is found in the crossover region ($\sigma \sim 10^{-4}$ mho/ \square) where small (5%) effects can be seen due to carrier heating. We emphasize that our concern here is with the gross transition from "metallic" to strongly localized behavior.

B. Low-temperature conductivity versus frequency

The far-infrared conductivity from $5-50 \text{ cm}^{-1}$ at the electron densities of interest are shown in Fig. 4. Qualitatively, they exhibit behavior that is expected. At metallic densities the conductivity relaxes in a Drude fashion whereas at the lowest electron densities the conductance exhibits a maximum at finite frequency. The dc values taken from Fig. 3 are indicated at zero frequency.

We also show in Fig. 5 the variation of $\sigma'(\omega)$ at the lowest density 6×10^{10} with substrate bias. The results are eminently sensible. Increasing substrate bias, which forces the electrons closer to the interface, causes the peak in the conductance versus frequency to shift and broaden to higher frequencies. The apparent loss of integrated absorption as the substrate bias is increased is not understood. Since the integrated intensity is directly proportional to the electron density we must conclude that there is more weight in the high-frequency tail outside the recorded range at large substrate bias.

IV. DISCUSSION

A comparison between theory and experiment was erected in the following manner. We have taken two cases, $g_s g_v = 4$ and $g_s g_v = 2$. The latter is motivated by recent suggestions that at low densities the valley degeneracy may be lifted,^{20,21} U and q_0 are fixed, and the best fit to $\sigma(T)$ is obtained by adjusting n_s for each set of data in Fig. 3. In this way good fits can be achieved for both $g_s g_v = 2$ and $g_s g_v = 4$ but a meaningful fit requires an n_s close to the experimental one.

In Figs. 6 and 7 we display the extent that agreement can be achieved with U and q_0 fixed. We have focused on the region below 4.2 K. At elevated temperatures increased electron-phonon scattering will change the conductance in a manner that is not included in the theory. (In this regard we note that the theory does not include phonon-assisted hopping at low temperatures. To the extent that the theory is successful we may safely neglect hopping.) Note that satisfactory agreement

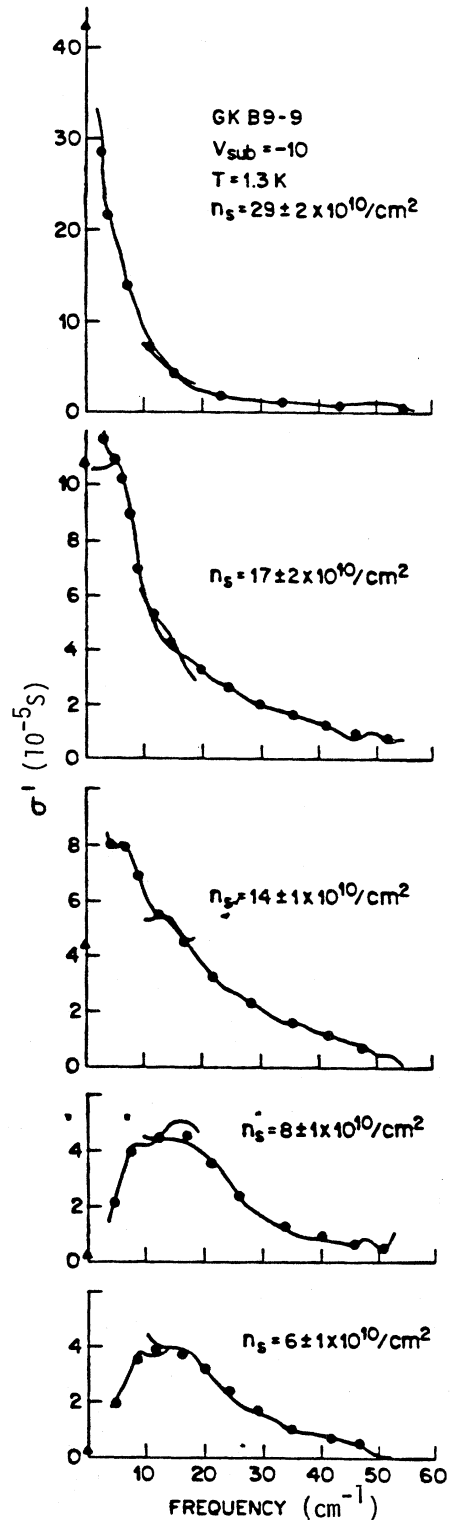


FIG. 4. Experimental $\sigma(\omega)$ with n_s as a parameter $T = 1.2 \text{ K}$. \bullet denote points used in the Kramers-Kronig analysis for Fig. 10. The two solid lines are different pieces of data obtained with a Michelson interferometer with different beamsplitters.

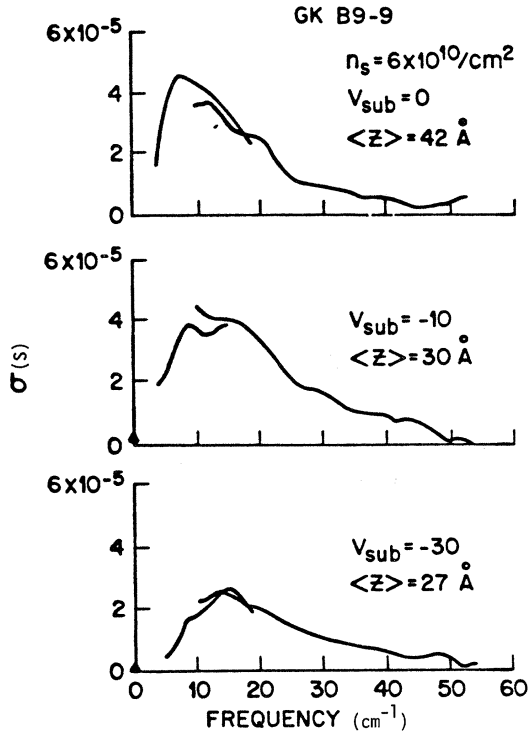


FIG. 5. Experimental $\sigma'(\omega)$ for $n_s \sim 6 \times 10^{10}/\text{cm}^2$ at $T = 1.2$ K with negative substrate bias as a parameter. The two solid lines are different pieces of data obtained with a Michelson interferometer with different beam-splitters.

is obtained in Fig. 6, for $g_s g_v = 4$, only with values of n_s that deviated significantly from experiment. The fit will be further compromised shortly when we compare with $\sigma(\omega, T \approx 0)$. However, Fig. 7 with $g_s g_v = 2$ exhibits a reasonable fit with values of n_s in close agreement with the experimental values.

In Figs. 8 and 9 we show the resulting $\sigma'(\omega, T = 0)$ for $g_s g_v = 4$ and $g_s g_v = 2$. It is clear that assuming $g_s g_v = 2$ gives much better overall agreement with experiment. If we focus our attention on $g_s g_v = 2$ we note that excellent agreement is obtained at the metallic and localized limits. (Note that the only parameter that is varied between these two extremes is the electron density.) The least satisfaction is obtained for $n_s = 14 \times 10^{10}/\text{cm}^2$.

We can compare experiment and theory at yet another level. By performing a Kramers-Kronig analysis on $\sigma'(\omega)$ we can obtain $\sigma''(\omega)$, the imaginary part. With the real and imaginary parts of σ one can simply invert Eq. (1) to obtain the real and imaginary parts of the memory function. Although, in principle, it contains no new informa-

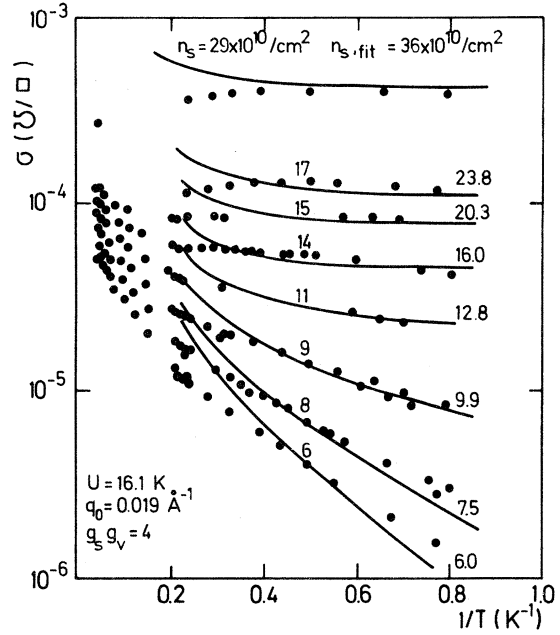


FIG. 6. Fit of σ vs $1/T$ assuming $g_s g_v = 4$. $U = 16.1$ K, $q_0 = 0.019 \text{ \AA}^{-1}$.

tion, it allows a direct comparison with the central quantity in the theory—the frequency-dependent memory function.

The imaginary part of σ, σ'' is shown in Fig. 10. This is obtained by a Kramers-Kronig analysis as-

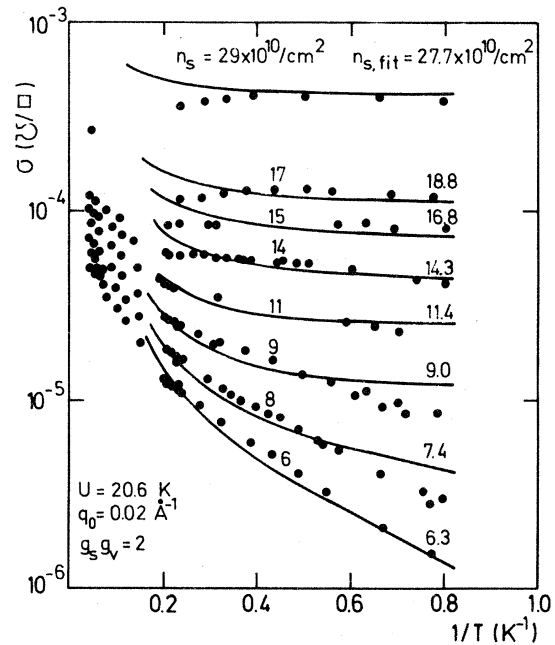


FIG. 7. Fit of σ vs $1/T$ assuming $g_s g_v = 2$. $U = 20.6$ K, $q_0 = 0.02 \text{ \AA}^{-1}$.

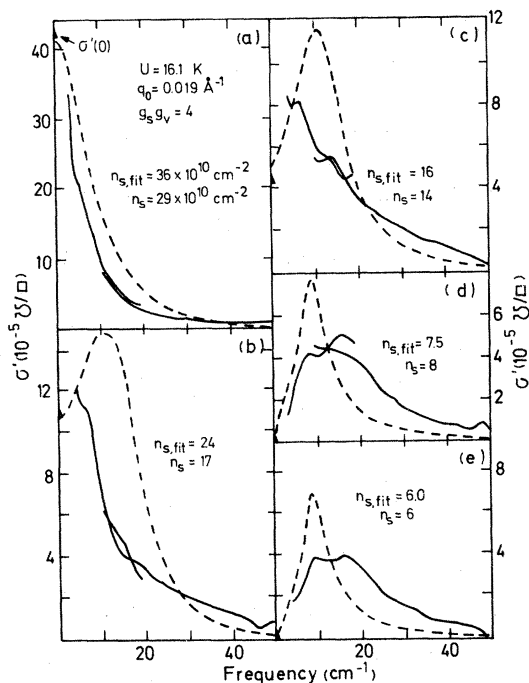


FIG. 8. Experimental $\sigma'(\omega)$ with n_s as a parameter —. — — $\sigma'(\omega, T=0)$ with parameters that produced Fig. 6. $g_s g_v=4$.

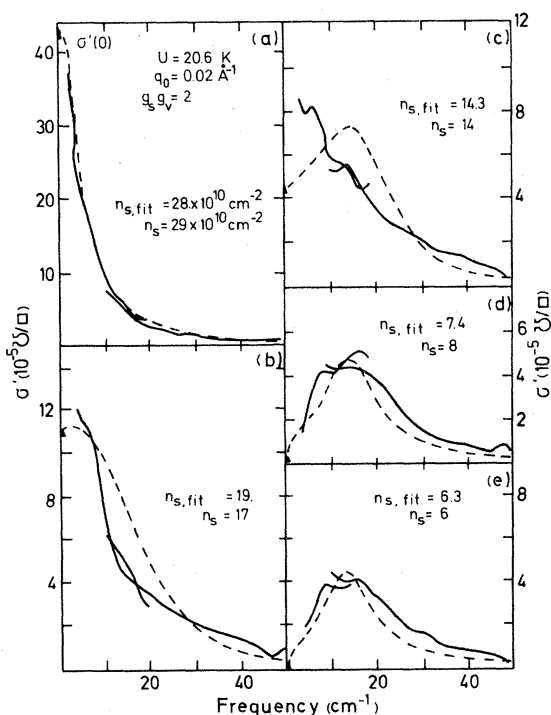


FIG. 9. Experimental $\sigma'(\omega)$ with n_s as a parameter —. — — shows $\sigma'(\omega, T=0)$ with parameters that produced Fig. 7, $g_s g_v=2$. $U=20.6$ K, $q_0=0.02$ \AA^{-1} .

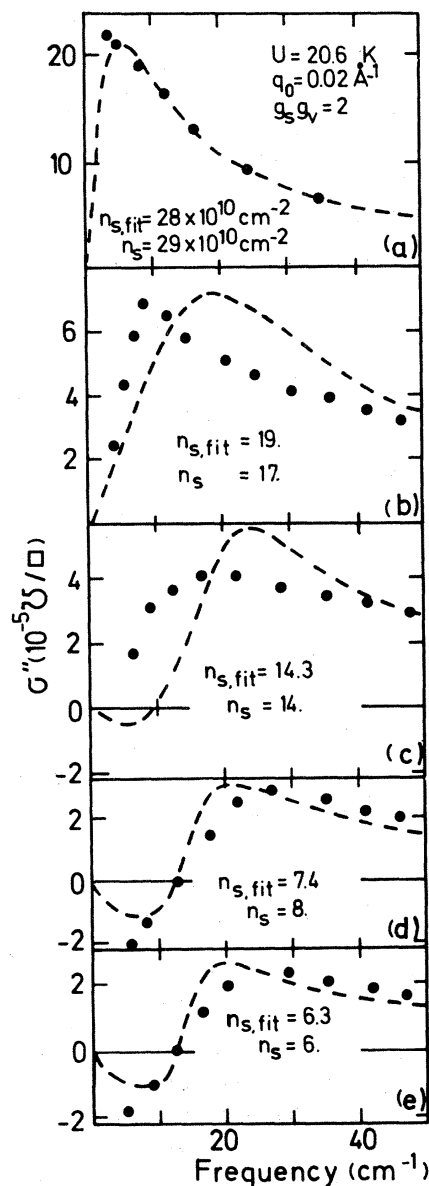


FIG. 10. Experimental imaginary $\sigma''(\omega)$ with n_s as parameter \bullet . Imaginary $\sigma(\omega, T=0)$ with parameters that produced Fig. 7. $g_s g_v=2$ — — —.

suming a piecewise linear interpolation of σ' between all points except $\omega=0$ and the first which is interpolated by

$$\sigma'(\omega) = \sigma'(0) + [\sigma'(\omega_1) - \sigma'(0)]\omega^2/\omega_1^2 \quad (7)$$

and the last point and $\omega = \infty$ which is extrapolated by

$$\sigma'(\omega) = \sigma'(\omega_N)(\omega_N^2/\omega^2). \quad (8)$$

Also shown in Fig. 10 is the imaginary conductivity derived from the fits for $g_s g_v=2$.

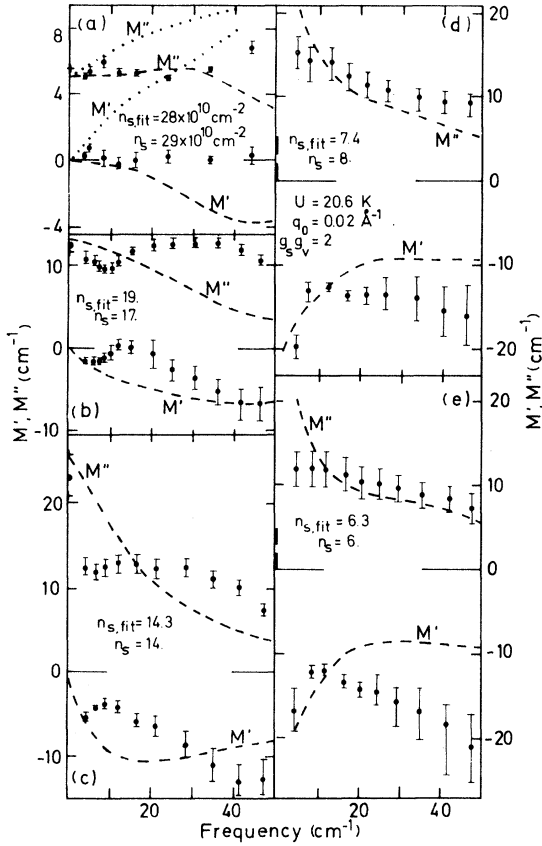


FIG. 11. Experimental real and imaginary $M(\omega)$ represented by bars. Real and imaginary memory function with parameters that produced Fig. 7. $g_s g_v = 2$, — — — $M(\omega)$ for Coulomb scatterers without demanding self-consistency. See Refs. 21 and 22, ····.

In Fig. 11 we finally show the real and imaginary memory function determined from the experimental data and compared with that generated by the theory. The error bars on the experimental data include only the uncertainty that is produced by uncertainties in the electron density. Again the most serious discrepancies are seen at $n_s \sim 14 \times 10^{10}/\text{cm}^2$ with satisfactory agreement achieved at the metallic and localized limits. Clearly the percentage errors in our measurements at high frequency ($> 30 \text{ cm}^{-1}$) are great than at intermediate frequencies ($10\text{--}20 \text{ cm}^{-1}$). Consequently we may expect some systematic errors to appear as we move into the high-frequency region. However, we have made no attempt to estimate these anticipated errors. We note that for $n_s = 29 \times 10^{10}/\text{cm}^2$ there is excellent agreement between theory and experiment for $\sigma'(\omega)$ and $\sigma''(\omega)$ [Figs. 9(a) and 10(a)]. However, there exist deviations in $M'(\omega)$ and $M''(\omega)$, as can be seen from

Fig. 11(a).

In Fig. 11(a) we also show results calculated according to the theory of Ganguly and Ting²² and Tzoar, Platzmann, and Simons²³ which make no attempt at self-consistency and are based on charged impurity scattering. The theory deviates in the opposite direction and is less satisfactory.

The n_s dependence of $1/M''(\omega=0) \equiv \tau$ (τ is the Drude relaxation rate) is shown in Fig. 12 with U and q_0 as in Fig. 7. The arrows indicate the n_s values which produce Fig. 7. Because τ goes continuously to zero for $n \rightarrow n_c$ (n_c is the critical density) the dc conductivity

$$\sigma(\omega=0, T=0) = \frac{n_s e^2}{m} \tau$$

also goes to zero continuously for $n \rightarrow n_c$.

In Fig. 13 we show a fit of some old data¹⁶ on Si(100) inversion layer surface. After the comments in Sec. III, we have only used the $\sigma(\omega, T=0)$ data for the fit. U and q_0 are kept fixed and only the density is varied to trigger the metal-insulator transition. However, here we obtain the best agreement if we use $g_s g_v = 4$. This is also consistent with recent suggestions^{20,21} that at high density the exchange correlation effects will not lift the valley degeneracy. However, since the reliability of the corresponding $\sigma(T, \omega=0)$ is in doubt we cannot make a convincing case for the applicability of the theory with this data.

From Table I, we can calculate the mean distance of the fixed oxide charges $q_I = (4\pi^3 n_{\text{FOC}})^{1/2}$, where n_{FOC} is the density of the fixed oxide

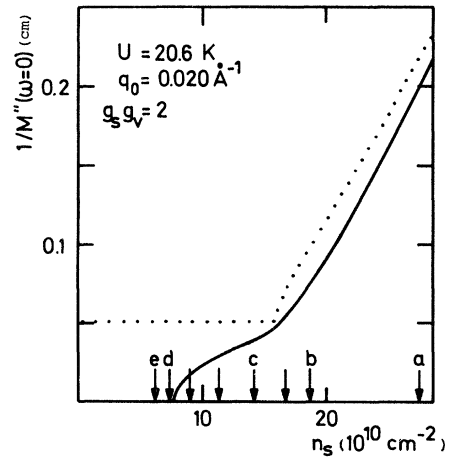


FIG. 12. n_s dependence of $1/M''(\omega=0)$ — — —, Boltzmann equation result ····, see Ref. 10; the arrows give $n_{s,\text{fit}}$, which produce Fig. 7.

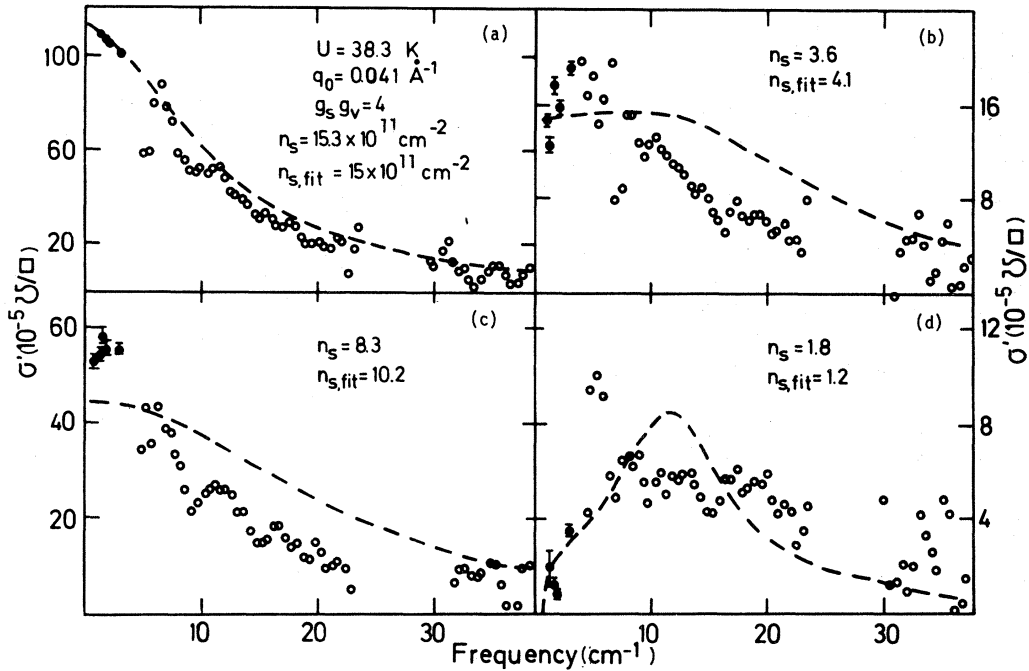


FIG. 13. Experimental $\sigma'(\omega)$ with n_s as a parameter after Allen, Tsui, and DeRosa (Ref. 16) \circ , $\sigma'(\omega, T=0)$ with $U=38.3$ K and $q_0=0.041 \text{ \AA}^{-1}$.

charge. A comparison between q_I and q_0 , given in Table II, shows that these two lengths are nearly equal. It must be noted, however, that fixed charge at the interface would give a disordering potential $U(q)$ at least an order of magnitude larger than assumed here. Indeed at low densities any fixed charge located at the interface would be screened by a bound electron that would be trapped on it with binding energies of the order of 20 meV. We also include in Table II the critical density $n_{c,fit}$ at which the metal-insulator transition occurs. So, for sample no. 1 only two experimentally measured $\sigma'(\omega)$ are near the critical density: $n_s=6 \times 10^{10} \text{ cm}^{-2}$ and $n_s=8 \times 10^{10} \text{ cm}^{-2}$. For sample no. 5 only the lowest density $n_s=18 \times 10^{10} \text{ cm}^{-2}$ is near $n_{c,fit}$.

TABLE II. Random potential length scale.

Sample	q_I ($1/\text{\AA}$)	q_0 ($1/\text{\AA}$)	$n_{c,fit}$ $\times 10^{10} \text{ cm}^{-2}$
1	0.022	0.020	7.67
5	0.035	0.041	13.54

V. CONCLUSION

We have compared the self-consistent current-relaxation theory for strongly disordered systems with measured temperature- and frequency-dependent conductivities of n inversion layers on Si(100) surfaces. Quantitative agreement is achieved for fixed disordering potential strength and range provided that the valley degeneracy is lifted. Under these conditions the theory gives good account of the transition to strong or exponential localization as electron density is varied. The frequency-dependent conductivity exhibits a precursor to the metal-insulator transition by developing a maximum at finite frequency as the density approaches the critical density.

ACKNOWLEDGMENTS

One of the authors (A. G.) wishes to thank Dr. W. Götze for many discussions and expresses his sincerest thanks to the Friedrich-Ebert-Stiftung for a grant. The experimental effort benefited from the technical support of G. Kaminsky and F. DeRosa.

- ¹W. Götze, *Solid State Commun.* **27**, 1393 (1978).
- ²W. Götze, *J. Phys. C* **12**, 1279 (1979).
- ³W. Götze, *Philos. Mag. B* **43**, 219 (1981).
- ⁴D. Belitz and W. Götze, *Philos. Mag. B* **43**, 517 (1981).
- ⁵E. Abrahams, P. W. Anderson, D. C. Licciardello, and T. V. Ramakrishnan, *Phys. Rev. Lett.* **42**, 673 (1979).
- ⁶G. J. Dolan and D. D. Osheroff, *Phys. Rev. Lett.* **93**, 721 (1979).
- ⁷D. J. Bishop, D. C. Tsui, and R. C. Dynes, *Phys. Rev. Lett.* **44**, 1153 (1980).
- ⁸D. Vollhardt and P. Wölfle, *Phys. Rev. B* **22**, 4666 (1980).
- ⁹D. Vollhardt and P. Wölfle, *Phys. Rev. Lett.* **45**, 842 (1980).
- ¹⁰A. Gold and W. Götze, *J. Phys. C* **14**, 4049 (1981).
- ¹¹S. Pollit, M. Pepper, and C. J. Adkins, *Surf. Sci.* **58**, 79 (1976).
- ¹²C. J. Adkins, S. Pollit, and M. Pepper, *J. Phys. (Paris) C* **4**, 343 (1976).
- ¹³D. C. Tsui and S. J. Allen, Jr., *Phys. Rev. Lett.* **32**, 1200 (1974).
- ¹⁴M. Pepper, *Proc. R. Soc. London Ser. A* **353**, 225 (1977).
- ¹⁵F. Stern, *Phys. Rev. Lett.* **38**, 546 (1967).
- ¹⁶S. J. Allen, Jr., D. C. Tsui, and F. DeRosa, *Phys. Rev. Lett.* **35**, 1359 (1975).
- ¹⁷D. C. Tsui, S. J. Allen, Jr., R. A. Logan, A. Kamgar, and S. N. Coppersmith, *Surf. Sci.* **73**, 419 (1978).
- ¹⁸B. A. Wilson, S. J. Allen, Jr., and D. C. Tsui, *Surf. Sci.* **98**, 262 (1980); *Phys. Rev. Lett.* **44**, 479 (1980).
- ¹⁹B. A. Wilson, S. J. Allen, Jr., and D. C. Tsui, *Phys. Rev. B* **24**, 5887 (1981).
- ²⁰W. L. Bloss, L. J. Sham, and B. Vinter, *Phys. Rev. Lett.* **43**, 1529 (1979).
- ²¹T. Cole, B. D. McCombe, J. J. Quinn, and R. K. Kalia, *Phys. Rev. Lett.* **46**, 1096 (1981).
- ²²A. K. Ganguly and C. S. Ting, *Phys. Rev. B* **16**, 3541 (1977).
- ²³N. Tzoar, P. M. Platzmann, and A. Simons, *Phys. Rev. Lett.* **36**, 1200 (1976).